THE JOURNAL OF PHYSICAL CHEMISTRY C LETTERS

2008, *112,* 8132–8135
Published on Web 05/06/2008

Nature and Tunability of Enhanced Hydrogen Binding in Metal−Organic Frameworks with Exposed Transition Metal Sites

Wei Zhou*,†,‡ and Taner Yildirim†,§

NIST Center for Neutron Research, National Institute of Standards and Technology, Gaithersburg, Maryland 20899, Department of Materials Science and Engineering, University of Maryland, College Park, Maryland 20742, and Department of Materials Science and Engineering, University of Pennsylvania, Philadelphia, Pennsylvania 19104

Received: April 17, 2008

Metal−organic framework (MOF) compounds with exposed transition-metal (TM) sites were recently found to exhibit significantly larger experimental heats of adsorption of H_2 than classical MOFs, thus attracting greater attention. Here we show that the hydrogen binding in Mn_4Cl−MOF is not of the expected Kubas type because there is (a) no significant charge transfer from TM to H_2, (b) no evidence of any H_2-σ* Mn-*d* orbital hybridization, (c) no significant H−H bond elongation, and (d) no significant shift in H−H stretching mode frequency. We make predictions for the magnetic superexchange interactions in Mn_4Cl−MOF and determined low- and high-spin states of the Mn ion as local minima with very different hydrogen binding energies. We show that, by replacing Cl with F or Br, one can tune the H_2 binding energy. We further reveal that the major contribution to the overall binding comes from the classical Coulomb interaction which is not screened due to the open-metal site and explains the relatively high binding energies and short H_2−TM distances observed in MOFs with exposed metal sites compared to traditional ones. Finally, we show that the orientation of H_2 has a surprisingly large effect on the binding potential, reducing the classical binding energy by almost 30%.

Introduction

Metal−organic frameworks (MOFs) are a relatively new class of nanoporous materials that show great promise for hydrogen storage applications.[1] A serious impediment to MOF-based H_2 storage has been the unfavorably weak van der Waals (vdW) interactions that typically predominate between H_2 and the pore walls. Recently, MOF compounds with exposed transition metal (TM) sites[2,3] were found to have significantly larger heats of adsorption (∼10 kJ/mol) than classical MOFs (∼4−5 kJ/mol[4]), thus attracting greater attention. Understanding the nature of the enhanced H_2 interaction with the exposed transition metal sites is of critical importance for further improving the H_2−host binding in these materials.

H_2 binding and reactivity with transition metals has been an important topic of chemistry for many decades. Particularly relevant to hydrogen storage is the capability of transition metals and H_2 to form organometallic dihydrogen complexes (so-called "Kubas complexes") under certain circumstances, a fact well-known in transition-metal coordination chemistry.[5] In these complexes, the TM and H_2 form a nonclassical side-on bonding, with the H_2 binding strength determined by the type of TM and ligand. Electron donation from H_2-σ to TM-d coupled with electron back-donation from TM-d to H_2-σ* is essential to stabilize the TM−H_2 complex.[5] Importantly, by carefully choosing the TM and ligand, it is possible to design novel types of Kubas complexes and bring the TM−H_2 binding strength into the "appropriate" range, suitable for reversible H_2 adsorption/desorption under near ambient conditions. Indeed, it has been recently predicted that light transition metals affixed onto different nanostructures such as nanotubes, C_{60}, and small organic molecules could be potential H_2-storage systems with Kubas binding energies of 30−50 kJ/mol/H_2, which is compatible with room-temperature storage.[6]

Concerning MOFs with exposed transition metal sites, naturally, one may wonder if the enhanced H_2 binding with the TM shares the same origin as those found in Kubas complexes, and if so, why the observed heat of adsorption is only ∼10 kJ/mol, significantly smaller than a typical Kubas-type H_2 binding strength. Very recently, Sun et al. attempted to address this problem,[7] but none of the relevant indicators for Kubas-type interaction were considered. As mentioned above, charge transfer from H_2-σ to TM-d and electron back-donation from TM-d to H_2-σ* (i.e., the presence of a TM-d H_2-σ* antibonding orbital) are the key mechanism for Kubas-type interaction, and consequently, a significant elongation of the H−H bond and softening of the H_2 stretching mode should be observed. In this communication, using Mn_4Cl−MOF[2] as an example, we show that the hydrogen binding to the exposed transition metal sites in these MOFs is not of Kubas-type because none of the effects listed above are present. The special type of Kubas interaction suggested by Sun et al.[7] is problematic and should be clarified.

We also make predictions for the magnetic superexchange interactions in Mn_4Cl−MOF and determine low- and high-spin states of the Mn ion as local minima with very different hydrogen binding energies. We show that by replacing Cl with F or Br, one can tune the H_2 binding energy in this MOF system.

* Corresponding author. E-mail: wzhou@nist.gov.
† National Institute of Standards and Technology.
‡ University of Maryland.
§ University of Pennsylvania.

10.1021/jp803350y CCC: $40.75

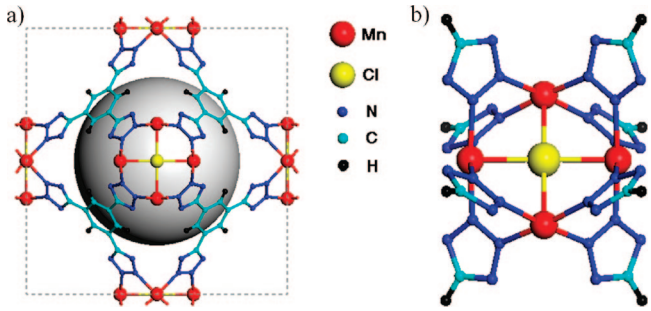

Figure 1. (a) Crystal structure of Mn_4Cl−MOF. The large sphere at the cell center illustrates the void space in the unit cell. (b) Mn_4Cl−MOF cluster, the key building block of the Mn_4Cl−MOF crystal, terminated with hydrogen atoms.

We further reveal that the major contribution to the overall binding comes from the classical Coulomb interaction, which is not screened due to the open metal site and explains the relatively high binding energies and short H_2−TM distances observed in MOFs with exposed metal sites compared to traditional ones. Finally, we show that the orientation of H_2 has a surprisingly large effect on the binding potential, reducing the classical binding energy by almost 30%.

Computational Methods

First-principles calculations were performed using plane-wave implementation of the generalized gradient approximation (GGA) to density functional theory (DFT) as implemented in the PWscf package.[8] Since our goal here is not to estimate the magnitude of the weak vdW interactions, it is appropriate to use GGA which gives accurate results for charge transfer, hybridization, phonons, Coulomb interaction, etc. We used a Vanderbilt-type ultrasoft pseudopotential with Perdew−Burke−Ernzerh exchange correlation, 410 eV cutoff energy and gamma point sampling. All atomic positions were optimized until the maximum forces on atoms are less than 0.01 eV/Å. The H_2 binding energy was calculated using $E_B = E(\text{MOF}+H_2) - E(\text{MOF}) - E(H_2)$. A negative E_B means that H_2 is bound to MOF. Additional details about our calculation are provided in the Supporting Information (SI).

Results and Discussion

We considered both the actual crystal structure and a simplified isolated cluster model (see Figure 1). Since the structure contains Mn, it is also important to consider various possible magnetic configurations and Mn spin states. Our calculations were done for ferro, antiferro, and dimer magnetic configurations and three orientations of the H_2 molecule as schematically shown in Figure 2. We considered both low ($S = 3/2$) and high spin ($S = 5/2$) states for the Mn ions. The results are summarized in Table 1.

From Table 1, we see that the simplified cluster model gives almost the same hydrogen binding energies as the full crystal structure and therefore is a good approximation for the Mn_4Cl−MOF system. Thus, from now on, we focus our discussion on the cluster structure, which is easier to read. The magnetic-coupled dimer configuration (Figure 2c) has always the lowest energy, indicating an antiferromagnetic superexchange interaction for the linear Mn−Cl−Mn bond (i.e., J_2). It is worth mentioning that the previous work by Sun et al. only considered the ferromagnetic configuration,[7] which is unfortunately not the ground-state magnetic configuration.

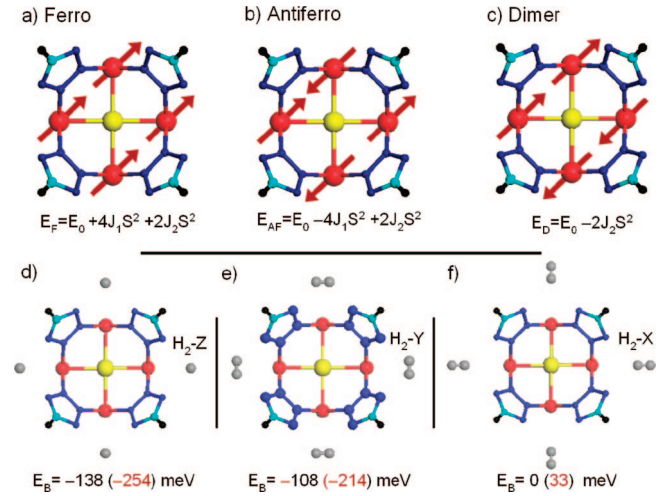

Figure 2. Top view of the Mn_4Cl-MOF cluster with three magnetic configurations and their energies in terms of nearest (J_1) and next-nearest (J_2) exchange interactions. Bottom panel shows H_2−Mn_4Cl−MOF cluster for three different H_2 orientations. The H_2 binding energies (E_B) and pure Coulomb contributions (in parentheses) are also given.

TABLE 1: Total Energy of the Bare Mn_4Cl−MOF (E_{Bare}) and the Binding Energies of an H_2 Molecule with Orientations along *Z*, *Y*, and *X*, respectively, as a Function of Three Magnetic Configurations (Figure 2) for Crystal and Cluster Models[a]

	E_{Bare} (eV)	$E_B(H_2)$ Z,Y,X (meV)	S, J_1, J_2 (meV)
ferro	−7.002	−138.1, −110.4, 0	crystal $S = 5/2$
AF	−7.065	−136.9, −109.3, 0	$J_1 = 1.35$
dimer	−7.147	−137.0, −109.2, 0	$J_2 = 4.55$
ferro	−5.172	−135.6, −105.9, 0	cluster $S = 5/2$
AF	−5.234	−134.3, −104.4, 0	$J_1 = 1.24$
dimer	−5.313	−137.8, −107.6, 0	$J_2 = 4.40$
ferro	−4.879	−79.0, −49.7, 0	cluster $S = 3/2$
AF	−4.636	−81.6, −52.8, 0	$J_1 = -13.5$
dimer	−5.023	−83.5, −53.9, 0	$J_2 = 29.5$

[a] H_2 bond length and H_2 stretching mode frequency. $d = 0.76$ (0.75) Å, $\omega = 4183$ cm^{-1} (4340 cm^{-1} for free H_2).

Surprisingly, the effect of magnetic configuration of the Mn_4Cl-MOF cluster on the H_2 binding energies is quite small. This is not the case for the spin state of the Mn ions where the high-spin state has about twice the H_2 binding energy as the low-spin state. Hence it is important to understand what controls the spin state of Mn ions in Mn_4Cl−MOF. We find that it is basically determined by the competition between the Hund rule (prefers high spin) and the crystal-field splitting of the Mn d-levels (prefers low spin) which is controlled by the Mn−X distance as shown in Figure 3a. It is possible to switch the magnetic ground-state of Mn ions from low to high spin by changing the halogen from X = F to X = Br, with X = Cl being near the midpoint (Figure 3a). The calculated H_2 binding energies for the z-orientation are 114 and 139 meV in the high-spin state and 77 and 81 meV in the low-spin state for X = F and X = Br, respectively. Hence assuming the true magnetic ground-state of Mn_4Cl-MOF is high-spin as predicted here, one may lower the binding energy significantly by simply replacing Cl with F. However, since magnetic energies are difficult to calculate accurately from pseudopotential methods, it is also quite possible that the X = Cl case may fall in the low-spin state of the phases shown in Figure 3a, in which case it would be possible to increase the H_2 binding energy significantly by simply replacing Cl with Br. In Table 1 and SI, we provide the magnetic exchange parameters and the energy levels for both

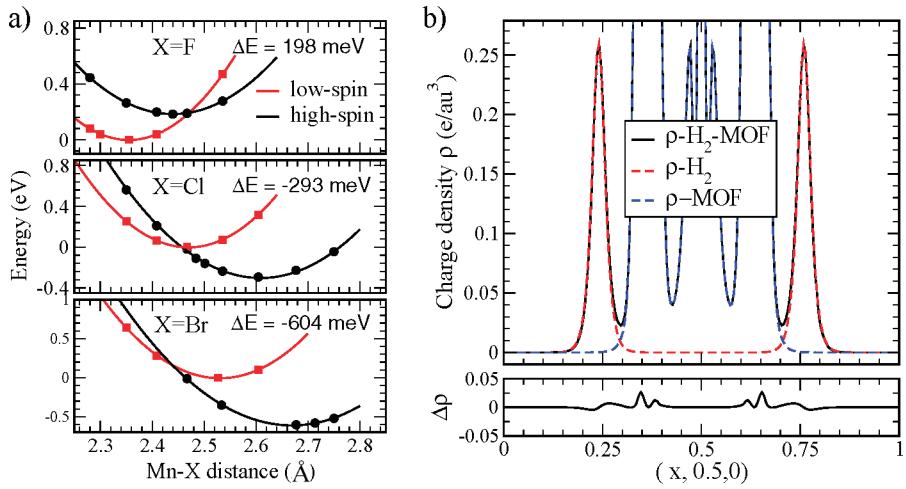

Figure 3. (a) Energy vs Mn−X distance curves in low (red) and high-spin (black) states, indicating transition from low-spin to high-spin ground-state as X goes from F to Br. (b) The calculated charge density along the x direction for H_2−Mn_4Cl−MOF (black) and the isolated subsystems (Mn_4Cl−MOF (blue) and H_2 (red)) and the difference plot (bottom panel).

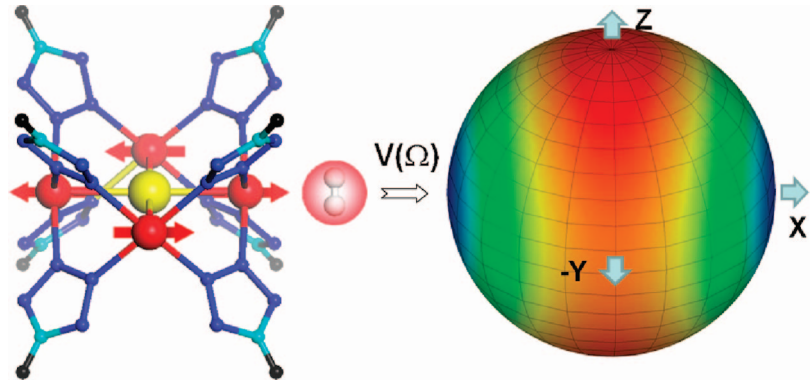

Figure 4. Contour plot of the orientation dependence of the binding energy of H_2 on Mn_4Cl−MOF cluster in (θ, φ) space. The red and blue regions represent strong and weak binding energy, respectively.

high- and low-spin models. This information will be invaluable in future experiments such as magnetization and neutron scattering to determine the true magnetic ground-state of Mn_4Cl−MOF. At any rate it would be interesting to synthesize new Mn_4X−MOFs with other halogens and measure the hydrogen heat of adsorption.

Concerning the nature of H_2-binding to metal sites, we did not find noticeable charge transfer between H_2 and Mn. Inspecting the molecular orbitals, we were not able to find an orbital which represents the TM−H_2 antibonding hybridization as found in other classical Kubas-type bindings. As an end effect, there is no significant H_2 bond elongation and only a small red shift in the H−H stretching mode (see Table 1). In fact, the charge density of the H_2−Mn_4Cl−MOF system can be well described by a direct superposition of the individual subsystems as shown in Figure 3b, further indicating the lack of strong chemical hybridization in this system. Hence all of these clearly indicate that the H_2−TM interaction in Mn_4Cl−MOF is not the previously suggested Kubas-type. Instead, we find that small charge overlap between H_2 and Mn_4Cl−MOF subsystems, as also shown in Figure 3b, results in significant attractive electrostatic interactions (given in parentheses in Figure 2) that explains not only the relatively large binding energy of H_2 in Mn_4Cl-MOF but also the observed small TM-H_2 distance that came out nicely in our calculations (see SI for details). Of course, the attractive Coulomb interaction is balanced by van der Walls type repulsive interaction, which makes the overall binding energy roughly half of the magnitude of the Coulomb contribution.

Probably one of the most striking findings given in Table 1 is the very different H_2 binding energies for three different orientations. Such a strong orientation-dependent potential is reminiscent of the two-dimensional quantum rotor state of hydrogen molecules adsorbed on step atoms on a Cu surface.[9] We note that the center of mass (CM) of the H_2 molecule strongly depends on the orientation of the H_2 molecule. For simplicity, here we present results of the orientational dependence of the potential without coupling to the CM. We have performed single-energy calculations for about 20 × 20 grid points in (θ, φ)-space and then used two-dimensional cubic-spline to get the potential energy at a given arbitrary angles. We expanded the potential in terms of spherical harmonics (Y_l^m) and estimated the orientational potential to be $V(\Omega) = V_0 + a_{20}Y_{20}(\Omega) + a_{22}(Y_2^2(\Omega) + Y_2^{-2}(\Omega))$, which mixes rotational levels up to $J = 6$ and yields ground-state energies $\langle E_B \rangle \sim -101$ and −55 meV for high and low-spin states, almost a 30% reduction from the classical values (see SI for details). As shown in Figure 4, the rotational dynamics of H_2 is strongly confined to a narrow slab-like region (the red region). Full analysis of hydrogen quantum dynamics in Mn_4Cl-MOF is beyond the scope of this communication and will be discussed elsewhere. Here we just note that one should not compare the classical binding energies with the experimental heats of adsorption, which is unfortunately commonly done in the literature. As we found here, it is important to consider the H_2 rotational states in order to determine the actual binding energy.

Finally, we repeated some of the calculations for isostructural Cu_4Cl-MOF and obtained similar results (see SI for details).

Briefly, the H_2 binding energies (−66.6, −35.0, and −4.1 meV for *Z*, *Y*, and *X* orientations) are again very anisotropic and compare well with those of the low-spin state Mn_4Cl−MOF rather than the high-spin state. This suggests that the ground-state of Mn_4Cl−MOF could be the low-spin state and the hydrogen binding energy can be increased by Br substitution.

Conclusion

In summary, we have used Mn_4Cl−MOF as an example to elucidate several key issues concerning the enhanced H_2 binding found in MOFs with exposed transition metal sites. We have clarified that in Mn_4Cl−MOF, the H_2 binding to the exposed Mn sites is not of the expected Kubas-type. We also find no significant effect of the magnetic state of the Mn_4 cluster on the binding energy. However, the spin state of the Mn ion has a strong effect on the H_2 binding and can be tuned from low- to high-spin state by replacing Cl with F and Br, respectively. We reveal that the major contribution to the overall binding is due to the classical Coulomb interaction arising from small charge overlap of H_2-σ and Mn-d orbitals. This Coulomb interaction is very anisotropic, and when the quantum nature of H_2 orientation is taken into account, the actual binding energy is significantly reduced from the calculated classical binding energy. We hope that the predictions that we report in this study for the magnetic ground-state of Mn_4X−MOF and its dependence on other halogens with significant anisotropic H_2-binding energy will motivate further experimental studies on MOF materials with exposed metal sites.

In terms of general implications for hydrogen storage, our results suggest that enhancing the Coulomb interactions between H_2 and the pore surfaces is indeed a feasible route for improving the H_2 binding in physisorption-based storage systems. In addition to the MOF system studied in this work, recently observed, enhanced H_2 uptake in chemically reduced MOF materials[10] seems to further support this. However, an enhanced Coulomb interaction itself is not likely enough to bring the working temperature of physisorption system from cryogenic temperature all the way up to room temperature. Introducing a true Kubas-type structural motif into porous materials holds higher potential for accomplishing this and should continue to be pursued actively.

Acknowledgment. This work was partially supported by DOE BES Grant No.DE-FG02-98ER45701. The authors thank C. M. Brown, Y. Liu, R. L. Cappelletti, and T. J. Udovic for helpful discussions.

Supporting Information Available: Details of the DFT calculations, optimized atomic positions, and magnetic energy levels. This material is available free of charge via the Internet at http://pubs.acs.org.

References and Notes

(1) (a) Rowsell, J. L. C.; Millward, A. R.; Park, K. S.; Yaghi, O. M. *J. Am. Chem. Soc.* **2004**, *126*, 5666–5667. (b) Wong-Foy, A. G.; Matzger, A. J.; Yaghi, O. M. *J. Am. Chem. Soc.* **2006**, *128*, 3494–3495.

(2) Dinca, M.; Dailly, A.; Liu, Y.; Brown, C. M.; Neumann, D. A.; Long, J. R. *J. Am. Chem. Soc.* **2006**, *128*, 16876–16883.

(3) Dinca, M.; Han, W. S.; Liu, Y.; Dailly, A.; Brown, C. M.; Long, J. R. *Angew. Chem., Int. Ed.* **2007**, *46*, 1419–1422.

(4) Zhou, W.; Wu, H.; Hartman, M. R.; Yildirim, T. *J. Phys. Chem. C* **2007**, *111*, 16131–16137.

(5) Kubas, G. J. *Chem. Rev.* **2007**, *107*, 4152–4205.

(6) (a) Yildirim, T.; Ciraci, S. *Phys. Rev. Lett.* **2005**, *94*, 175501. (b) Yildirim, T.; Iniguez, J.; Ciraci, S. *Phys. Rev. B* **2005**, *72*, 153403. (c) Zhao, Y.; Kim, Y.-H.; Dillon, A. C.; Heben, M. J.; Zhang, S. B. *Phys. Rev. Lett.* **2005**, *94*, 155504. (d) Durgun, E.; Ciraci, S.; Zhou, W.; Yildirim, T. *Phys. Rev. Lett.* **2006**, *97*, 226102. (e) Zhou, W.; Yildirim, T.; Durgun, E.; Ciraci, S. *Phys. Rev. B* **2007**, *76*, 085434. (f) Phillips, A. B.; Shivaram, B. S. *Phys. Rev. Lett.* **2008**, *100*, 105505.

(7) Sun, Y. Y.; Kim, Y.-H.; Zhang, S. B. *J. Am. Chem. Soc.* **2007**, *129*, 12606–12607.

(8) Baroni, S.; Dal Corso, A.; de Gironcoli, S.; Giannozzi, P.; Cavazzoni, C.; Ballabio, G.; Scandolo, S.; Chiarotti, G.; Focher, P.; Pasquarello, A.; Laasonen, K.; Trave, A.; Car, R.; Marzari, N.; Kokalj, A. Quantum-ESPRESSO, V3.0; http://www.pwscf.org/.

(9) Svensson, K.; Bengtsson, L.; Bellman, J; Hassel, M.; Persson, M; Andersson, S. *Phys. Rev. Lett.* **1999**, *83*, 124.

(10) Mulfort, K. L.; Hupp, J. T. *J. Am. Chem. Soc.* **2007**, *129*, 9604–9605.

JP803350Y